Journal Pre-proof

Ultra-high throughput microfluidic concentrator for harvesting of Tetraselmis sp. (Chlorodendrophyceae, Chlorophyta)

Fateme Mirakhorli, Sajad Razavi Bazaz, Majid Ebrahimi Warkiani, Peter J. Ralph

PII: S2211-9264(23)00178-9

DOI: https://doi.org/10.1016/j.algal.2023.103145

Reference: ALGAL 103145

To appear in: *Algal Research*

Received date: 30 January 2023

Revised date: 1 May 2023

Accepted date: 11 May 2023

Please cite this article as: F. Mirakhorli, S.R. Bazaz, M.E. Warkiani, et al., Ultra-high throughput microfluidic concentrator for harvesting of Tetraselmis sp. (Chlorodendrophyceae, Chlorophyta), *Algal Research* (2023), https://doi.org/10.1016/j.algal.2023.103145

Ultra-high throughput microfluidic concentrator for harvesting of *Tetraselmis* sp. (Chlorodendrophyceae, Chlorophyta)

Fateme Mirakhorli[1*], Sajad Razavi Bazaz[2], Majid Ebrahimi Warkiani[2], Peter J Ralph[1*]

[1]Climate Change Cluster (C3), Faculty of Science, University of Technology Sydney, Australia

[2]School of Biomedical Engineering, University of Technology Sydney, Sydney, NSW 2007, Australia

Abstract

Microalgae are of commercial interest for their ability to produce high-value compounds and their potential to be used as feedstock across numerous industries. The production of algal biomass and other algal-based products involves different upstream and downstream processing steps, including cultivation, harvesting, and extraction. In particular, the harvesting process involves the extraction of a condensed algal slurry from a watery growth medium. This process accounts for 20 to 30% of the biomass production costs, creating technological and economic barriers. The conventional harvesting methods suffer from high costs, cross-contamination, and low yield. This study explores the use of a microfluidic technique, in particular, the rigid spiral microchannel, for ultra-high-throughput algae harvesting. We have designed a novel spiral channel that enables microalgae separation at high flow rates and spatial resolution, taking advantage of inertial microfluidic principles. The results from trials with surrogate microparticles and algal cells reveal that the microchannel has the potential to operate at 12 mL/min with separation efficiency >99%. Our inertial microfluidic device operates at high flow rates as a single channel, can be multiplexed, and shows excellent potential for large-scale processing of microalgae cultures. In addition, the lower number of loops provides the system with reduced back pressure, making it more desirable for operation using a range of different pumps. Since the overall cost of microalgae dewatering is substantial at the industrial scale, the design and fabrication of low-cost devices are of great importance, similar to the one we have developed in this study.

Keywords: *Microfluidics, algae dewatering; spiral microfluidics*

1 Introduction

Microalgae are of commercial interest for their ability to produce high-value compounds [1, 2] and their potential to be used as a feedstock across numerous industries [3]. Microalgae are phototrophic microorganisms with a 10-fold photosynthetic efficiency compared to terrestrial plants [4]. Having minimum (or no) requirement of arable land and relatively low costs of large-scale cultivation are characteristics of algae that make them favourable for industrial use [5]. The production of algal biomass and other algal-based products incorporates a number of different processing steps, including cultivation, harvesting, and extraction [6]. In particular, harvesting requires the retrieval of a condensed algal slurry from a watery growth medium [7]. Due to the small size of microalgae cells, ranging from 4 to 100 µm, and growing in a diluted suspension, the harvesting process is technically challenging. This process accounts for 20 to 30% of the entire biomass production cost, creating technological and economic barriers [8, 9].

Harvesting techniques are classified based on their working principle into either physical, chemical, electrical, biological, or magnet-based methods [10]. Physical harvesting processes include sedimentation, filtration, and centrifugation, where there is less chance of contamination, thereby leading to higher quality products and the possibility of reusing the growth medium. The high costs associated with physical methods, however, makes them economically undesirable. Despite the relatively high recovery efficiency of non-physical techniques such as flocculation (chemical), bioflocculation (biological), and electroflocculation (electrical), there is a high risk of contamination and toxicity to the cells. Magnetophoretic harvesting is a new approach with advantages over traditional harvesting techniques, such as high efficiency and short processing time. This method is expensive with potential metal contamination and not favorable for large-scale applications. These harvesting techniques have been primarily tested in laboratories, and their large-scale outdoor

amenability is yet to be assessed [10]. Therefore, there is a need for the development of a sustainable harvesting technique with minimal environmental impact and maximum harvesting efficiency.

Microfluidic technology has been shown to be a promising tool for the separation or concentration of microparticles or cells based on their size and morphology [11]. Microfluidic platforms can be operated by an external force (active) or by hydrodynamic forces (passive) generated within the microchannels, enabling precise manipulation of microparticles or cells [12]. Among all microfluidic devices, inertial microfluidic platforms are best for large-scale operations due to their intrinsic nature to operate at high flow rates [13]. The operation of inertial microfluidic systems is based on the inertial lift and Dean forces (in non-straight channels) generated by fluid movement within channels leading to two possible kinetic and equilibrium separations [14]. Particles inside a curved microfluidic channel experience different forces, which are dependent on the particle size, position, channel dimension, and fluid velocity [14]. The inertial lift and Dean drag forces are responsible for focusing and migration of particles to different equilibrium positions within the channel cross section. Inertial microfluidics offers a wide range of applications such as flow cytometry, mixing and optofluidic, filtration, separation, and concentration [15-17].

Recently, microfluidics has been considered a promising approach for microalgae-related applications [18]. Cell identification [19], sorting [20, 21], screening [22, 23], culturing [24, 25], and content extraction [26, 27] are important processes investigated within a microchannel. Dewatering, in particular, is important to perform either through microfluidic techniques as a pre-processing or post-processing step. However, few published data in the literature focus on microalgae dewatering using inertial microfluidics. In 2016, a trilobite-structure microfluidic device was introduced as a pre-concentrator for microalgae harvesting [28]. This study tested three different microalgae species at the optimum flow rate of 2

mL/min with about 30% efficiency for flexible live microalgae (*R. baltica* cells with no rigid cell wall considered as flexible cells) cells and 58% efficiency for smaller non-flexible samples (fixed cells and diatoms (*Chaetoceros* sp.) were considered as rigid non-flexible cells). Wang et al., (2017), developed an inertial microfluidic channel for harvesting cyanobacteria with a maximum recovery efficiency of 98.4% [29]. Currently in the literature, the maximum operational flow rate reported in this study was 700 µL/min, at which samples were concentrated by a factor of 3.2. The maximum operational flow rate for microalgae concentration was 20 mL/min using a multi-core inertial microfluidic device consisting of 4 spiral channels stacked [30]. However, according to the data shown in this study, there was significant defocusing at flow rates higher than 14 mL/min, and the optimum separation efficiency was only about 80%. Despite the recent improvements in microfluidic technology, the balance between throughput and separation efficiency is missing in the literature, i.e., devices with high throughput have low separation efficiency and vice versa.

In this study, we have proposed a robust microfluidic device to harvest microalgae *Tetraselmis* sp. with exceptionally high throughput and high efficiency that was suitable for either microalgae pre-concentration or harvesting. We have designed a novel spiral channel that enables microalgae separation at high flow rates and high spatial resolution, taking advantage of inertial microfluidic principles. Our inertial microfluidic device operates at high flow rates as a single integrated channel, thereby showing great potential for large-scale processing of microalgae cultures. In addition, the reduced number of loops provides our system with lower back pressure, making it more desirable for operation with a range of pumps. Since the overall cost of microalgae dewatering on a large scale is substantial for the industry, the design and fabrication of a low-cost device are important.

2 Material and method

2.1 Device fabrication

In this study, the inertial microfluidic device was directly fabricated using stereolithography, a 3D printing process by which fine and complex geometries are fabricated in a short period [31]. To do so, the microfluidic channel was first designed and drafted using the CAD drawing software SolidWorks 2021. The 3D model (exported with STL format) was sliced in the Z direction by the Miicraft software with a specific thickness of 10 µm and then sent to the high-resolution DLP 3D printer (MiiCraft Ultra 50, Hsinchu, Taiwan) featuring 30 µm resolution in XY direction with 32 × 52 × 120 mm^3 printing area. The printed part was removed from the printer picker, rinsed with isopropyl alcohol (IPA), and dried thoroughly to remove any liquid resin residuals from the channels. The microfluidic channel was UV cured using a UV-curing chamber at 405±5 nm wavelength as a post-curing process. The open side of the channel facing toward the resin tank was then enclosed using a PMMA sheet covered by a double adhesive tape (ARclear, Adhesive Research) [32].

2.2 Device characterisation

Different sizes of fluorescent microparticles (Fluoresbrite Microspheres, Polysciences Inc, Singapore) were used to evaluate device performance. To avoid adhesion or non-specific binding of microbeads to tubing, fluorescently labeled microparticles of 5, 7, 10, and 15 µm were diluted in MACS buffer (PBS containing 2 mM EDTA and 0.5% BSA) (Miltenyi Biotec, Germany). To introduce the sample into the microfluidic device, an algal suspension was loaded into a 10 mL BD plastic syringe and this was mounted on a programmable syringe pump (Fusion 200, Chemyx, USA). The sample was injected into the devices at varying flow rates, from 2 to 12 mL/min. After the sample became stable at each flow rate, the particle trajectory was recorded using an inverted epifluorescence microscope (Olympus IX73 microscope, Olympus Inc., USA) equipped with a DP80 dual-chip CCD camera

(Olympus Inc., USA) or a high-speed camera (PHANTOM VEO-E 340L MONO) mounted on an inverted microscope (Olympus IX73 microscope, Olympus Inc., USA) (the acquisition was achieved using Phantom Camera Control (PCC)). The separation efficiency of the device was calculated using the following formula to assess the device performance quantitively [33]:

$$\text{Separation efficiency\% (SE\%)} = \frac{\text{No. of microparticles in the target outlet}}{\text{Total No. of microparticles}} \times 100 \qquad (1)$$

2.3 Data processing

To record the fluorescent streaks of moving microparticles, image analysis software (TechSmith Camtasia Studio Version 2021.0.7) was used after particles reached steady-state conditions. The recordings were then rendered uncompressed in AVI format at 30 fps. ImageJ (1.52i) was used for image processing.

2.4 Microalgae source and cultivation

The chlorophyte microalgae *Tetraselmis* sp. was obtained from Climate Change Cluster (C3) culture collection at the University of Technology Sydney (UTS). *Tetrasemis* sp. cells are single motile cells with an average length of 10 and a width of 14 µm. Cells were maintained in f/2 growth medium containing filtered sterilised seawater, subjected to a 16/8 h light/dark cycle with 80 µmol photons m^{-2} s^{-1} light intensity. The temperature of the culture room was kept at around 23 ˚C, and the culture was aerated with air.

2.5 Analytical methods

2.5.1 Cell counting using flow cytometry

After each experiment, cell density was enumerated using a flow cytometer (Cytoflex LX, Beckman Coulter, CA, USA) and gated by their green fluorescence. The chlorophyll-a fluorescence emission (690/50 nm) was induced by blue excitation of 488 nm wavelength. Cells were first separated by gating within a plot of forward scatter (FSC) versus side scatter (SSC). Then, to separate live cells from dead cells/debris, another plot of FSC by cell area

(FSC-A) to chl-a fluorescence was created. To standardise the instrument, fluorescence calibration beads (CytoFlex Daily QC beads, Beckman Coulter, CA, USA) were used [34].

2.5.2 Photosynthetic activity measurements

As an indicator of plant stress and to assess the photosynthetic activity of the microalgal cells, the quantum yield of PSII photochemistry was measured using a portable fluorometer (AquaPen-C, Photon Systems Instruments, Czech Republic). Immediately after each experiment, a 3 mL aliquot of cell cultures was collected in a cuvette and placed in the device chamber for Chl-a fluorescence emission measurement. The saturating pulse of red light (630 nm) with a maximum intensity of 1890 µmol m^{-2} s^{-1} was used to measure the quantum yield of PSII of the cells after 15 minutes of dark adaptation [35].

2.5.3 Regrowth ability

To investigate the cells' ability to re-grow after being processed by the microfluidic concentrator, samples were collected and returned to the same growth condition they were taken from initially. The cultures started at the same initial density of 30 cells/µL, and cells were counted using the Flow cytometer every two to three days after the inoculation, as described in section 2.4.1.

2.5.4 Motility analysis

To investigate the cell motility after passing through the microfluidic concentrator, we placed 10 µL of sample on a glass slide and inspected their movement with the bright-field microscope. Using the CCD camera, a thirty-second video of the cell movement was captured at the magnification of 40X. The footage was then processed using the TrackMate plugin of ImageJ. Maximum velocity and mean velocity of two random cells were then measured in both control and processed samples [36]. The data were then analysed using one-way ANOVA test to determine any significant change in cells' motion. To do so, the velocity of

the cells before and after going through the microfluidic channel were compared with a significance level of 95% [37].

3 Results and discussion

3.1 Theory and design principles

The working principle of the microfluidic channel is based on inertial focusing mechanisms described by hydrodynamic forces (lift and drag forces) acting upon cells and particles. In high-velocity flow fields, particles endure lift and drag forces and will eventually stand in an equilibrium position where there is a balance between these forces. Inertial lift and Dean drag forces are defined as follows:

$$F_L = \rho(\frac{U_{max}}{D_h})C_L a^4 \quad (2)$$

$$F_D = 5.4 \times 10^{-4}\pi\mu a De^{1.63} \quad (3)$$

Where a is the particle diameter, μ is viscosity, ρ is density, D_h is the channel hydraulic diameter, U_{max} is the maximum fluid velocity, which is approximately twice the average fluid velocity, De is Dean number, and C_L is a dimensionless coefficient of lift that is dependent on the Re (Reynolds) number.

In a straight channel, cells experience two forces: i). shear-induced lift force by which cells are pushed toward the channel wall, ii). wall-induced lift force by which cells are moved toward the channel centre. In curved channels (like a spiral), however, there is a mismatch of the velocity in the channel cross-section, leading to the creation of another force called the Dean drag force. In equation (2), De describes the strength of the Dean force, which is defined as the following equation:

$$De = Re\sqrt{\frac{D_h}{2R}} \quad (4)$$

Wherein R is the radius of the curvature. According to equations (1) and (2), inertial lift and Dean drag forces can scale with the cell diameter to the power of four ($\propto a^4$) and one ($\propto a$), respectively. This explains why particles of different sizes could be collected from different channel outlets [38].

3.2 Device characterization

To evaluate the performance and sensitivity of the microfluidic concentrator, the device has been first characterized with surrogate microparticles. To do so, particle sizes ranging from 5 to 15 µm have been tested at different flow rates. Fluorescence streaks shown in Fig. 2 are made from images taken by an inverted microscope, and then stacked using ImageJ. This figure illustrates each particle's focusing bands and distribution passing through the channel. At low flow rates of 2 and 4 mL/min, almost all particle sizes are evenly dispersed throughout the channel. By increasing the flow rates, particles with larger diameters experienced more significant inertial lift and Dean drag forces. Eventually, they occupied a stationary point where all forces were mathematically balanced (close to the channel's outer wall). The channel hydraulic diameter is ~ 186 µm (channel cross-section is trapezoidal with width of 600 µm and heights of 80 µm and 140 µm); in our previous publications [39, 40], we showed that rigid microchannels are able to focus particles larger than a ($a/D_h = 0.04$, a is particle size, D_h is channel hydraulic diameter). Therefore, the minimum particles being focused in the rigid spiral microchannels developed in this study is ~ 7 µm. As such, 5 µm particles are only affected by the Dean vortices and do not create a focused band toward the channel's outer wall. However, particle sizes of 7 µm and larger are affected by inertial and Dean drag forces. Based on the competition between these two forces, they occupy different equilibrium positions in the channel. Particles of 7 and 10 µm size are dispersed at 2 and 4 mL/min flow rates but then started focusing toward the outer outlet wall at higher flow rates of 6, 8, 10, and 12 mL/min. By increasing the flow rate, particles of 15

µm size experienced a gradual shift from the inner to the outer wall. Based on the actual application of this study, the channel was designed to focus particles of the same size as the actual *Tetraselmis* cells ranging from 5 to 15 µm size into one single position. As indicated by the normalised intensity profiles in Fig. 2A, particles of 7 µm and bigger size could be separated and focused at the outer outlet of the channel with a tight focusing band. This tight focusing band enabled us to design the channel with a higher ratio of inner outlet diameter to outer outlet diameter, leading to a better concentrating ratio.

To quantify the separation efficiency of each particle size at each flow rate, particles were collected from each outlet and enumerated by a flow cytometer using Eq. 1. As shown in Fig. 2B, the separation efficiency of a 5 µm particle is 75% at flow rates higher than 8 mL/min. The separation efficiency reaches 98% for 7 µm particles at a 12 mL/min flow rate. Particles larger than 7 µm were all separated at 12 mL/min flow rate with more than 99% efficiency. For the current microfluidic channel, 12 mL/min is the maximum functional flow rate, as higher flow rates cause pressure build-up. Consequently, the pump cannot work continuously, and the cell viability might be compromised. Results demonstrate the effectiveness of using our current microfluidic design for the concentration of microalgae cultures at a flow rate as high as 12 mL/min with a high degree of separation efficiency. The ability of the device to focus particles with a wide size range of 7-15 µm is also of interest, as it encompasses widely used microalgae species for different applications, such as *Schizochytrium* sp. (with an approximate size of 9-14 µm) for its Docosahexaenoic acid (DHA) and *Chlorella* (with an approximate size of 6-12) used for edible products.

3.3 Input cell density effects on the device performance

One necessity for the microfluidic concentrator is to concentrate different ranges of microalgae culture density successfully. To investigate the device's capacity for dewatering, we tested different initial microparticle densities and analyzed their effects on focusing and

separation efficiency. The microfluidic device was tested at the minimum initial density of 0.01% v/v and maximum initial density of 1% v/v with the following demonstration of inertial focusing performance. Fig. 3A shows the fluorescent streaks, normalised intensities (Fig. 3B), and overlayed-focusing images of particle movement (Fig. 3C) within the channel. The tight single focusing band corresponding to initial densities of 0.01% v/v (60,000 particles/mL), 0.1% v/v (600,000 particles/mL), and 1% v/v (6,000,000 particles/mL) from left to right, respectively, is depicted throughout the channel with a dashed line in which normalized intensity graphs are plotted. The normalised intensity graph shows the particle distribution based on their pixel intensity across the channel cross-section, and higher intensity regions indicate areas in the channel with the highest density of microparticles. The pink dashed line divides the targeted outlet from the waste outlet, showing the isolation region. By increasing the initial density of the microparticles, the normalised intensity peak remains in a similar position while the FWHM (full width at half maximum) increases. This increase in the profile width is also observed in overlayed-focusing images, meaning that the particle-particle interaction tends to increase. By increasing the particle interaction, particle trains start defocusing, and the recovery efficiency remains high as long as there is enough room in the isolation region for the particles to entrain. In this study, the device's capability to concentrate samples with no decrease in efficiency was estimated as high as 6×10^6 cell/mL. To increase the dewatering capacity, collected sample from the target outlet can be recirculated into the microfluidic device as a multi-step serial concentrating process.

3.4 Ultra-high throughput dewatering of *Tetraselmis* sp.

As discussed in the literature review section, one important limitation of microfluidic devices for microalgae dewatering and pre-concentration is their limited capacity in throughput and processing speed. Another challenge associated with upscaling microfluidic systems is the high pressure build-up resulting from increasing the flow rate. High-pressure build-up can

also be more challenging depending on the material used for device fabrication. For instance, typical PDMS (Poly(dimethylsiloxane))-made microfluidic devices are more susceptible to large deformations and failure during the separation process at high flow rates. In this study, we aimed to address some of the abovementioned issues to facilitate microfluidic use for large-scale algae dewatering/pre-concentration. The designed spiral microfluidic channel in this study is made of resin, a low-cost accessible material, with three loops to reduce back pressure. To demonstrate a successful application of microalgae dewatering, *Tetraselmis* sp. microalgae at its typical growth density was tested at flow rates of 2-12 mL/min with intervals of 2 mL/min. Fig. 4A shows the composite focusing of the microalgae cells distributed in the outlet bifurcation and their corresponding flow cytometry data. At a low flow rate of 2 mL/min, cells are scattered within the channel width primarily toward the bigger outlet (waste outlet). As shown in Fig. 4A, by increasing the flow rate, microalgae cells start moving from the inner wall toward the outer wall due to changes in inertial and drag forces. At high flow rates of 10 and 12 mL/min, the focusing position completely shifted from the inner wall toward the outer wall, where the inertial forces are balanced with drag forces. We next characterised the recovery efficiency (= number of microalgae cells collected from target outlet/ total number of microalgae cells) of the device at each flow rate. At 2 mL/min, cells were recovered with very low efficiency of average 13.5%, while this number had a sharp increase at 4 mL/min flow rate. Figure 4B and C shows that our microfluidic device is capable of concentrating microalgae samples at higher flow rates than 6 mL/min with high and stable performance. The recovery efficiency for flow rates of more than 6 mL/min is more than 90% where for flow rates of 10 and 12 mL/min, it reaches ~ 99%. Each flow rate has been repeated and tested three times, and small error bars indicate the device's reliability. Due to the high operational flow rate, microalgae cells are exposed to high shear stress while passing through the microchannels. To investigate effects of high shear stress,

maximum quantum yield (F_v/F_m) of the cells was measured as an indicator for cells' photosynthetic activity. The results of quantum yield measurement depicted in Fig. 4C show no significant impact on the photosynthetic activity of the microalgae cells after concentrating. Therefore, 12 mL/min has been selected as the optimal flow rate within this channel for algae dewatering.

3.5 Cell regrowth and motility analysis

We conducted further experiments to analyse the performance of microalgae after exposure to microchannels at a flow rate of 12 mL/min. The experimental setup has been demonstrated in Fig. 5A. The input sample of *Tetraselmis* sp., the target outlet, and the waste outlet are illustrated in Fig. 5B; as is evidenced, the sample colour of the target outlet becomes darker while the cell-free outlet sample colour is transparent, meaning the successful dewatering of algae cells at 12 mL/min. To further analyse the microchannel performance, the top view stacked images of the microalgae movement over 200 frames were illustrated in Fig. 5C. The loop-by-loop analysis illustrates that after the 1st loop, cells are perfectly aligned at the channel outer wall, moving from loop 2 to loop 4 which assists in making the focusing band of the cells even tighter. However, for this applications where the pressure-drop or the energy input is of great importance, our analysis identified that using our spiral microchannel with only 2 loops is enough to dewater this algae species.

Regrowth experiments were also performed to assess the impact of shear stress impacts on the cells' ability to grow after the microfluidic processing at the highest 12 mL/min flow rate. Growth curves shown in Fig. 5A revealed no significant difference between the control and processed samples. In addition, two random cells were targeted from each control and processed samples to investigate the possible effects of high shear stress on microalgae cells' motility. The motion of these four cells was recorded and quantified using ImageJ. As shown in Fig. 5F, the maximum velocity of cell 1 before the processing (BP1) is slightly higher than

the other cells. However, the average speed of the cells before (BP1 and BP2) and after processing (AP1 and AP2) remained the same (P value > 0.05). Fig. 5G and H also show similar trends for each of the two cells before and after processing by our microfluidic concentrator. Overall, as no significant change was found during the motion analysis, our microfluidic device is compatible with microalgae cells, and the microalgae cells can remain viable. Therefore, further post-processing and/or re-cultivation can be followed directly after microfluidic processing.

The performance of the spiral microchannel device compared to other existing microfluidic devices has been compared in Table 1. As shown in this table, various algae species have been concentrated within microfluidic devices. The benefit of our rigid spiral microchannel is that it can operate over a wide range of particle sizes, indicating it has the potential to dewater various algae species. More importantly, the proposed system is robust; the channels are made of rigid materials; hence, they do not suffer delamination or debonding, a common challenge in PDMS-made microchannels [41]. A single rigid spiral microchannel can operate at a flow rate as high as 12 mL/min, 6 times more than the Trilobite design, 40 times more than asymmetric serpentine, and 9.6 times more than the previously designed spiral microchannel. The separation efficiency of our system is also significant; we can dewater more than 99% of the algae cells, and only those that form clusters escape from the target outlet. We have previously shown the scaled-up version of the spiral microchannel [42]; therefore, by planar multiplexing, our system can operate as high as 48 mL/min (Fig. 6A) and by vertical multiplexing, our system can operate with a flow rate of more than 100 mL/min (Fig. 6B).

Table 1. Performance comparison of rigid spiral microchannel compared to other available microfluidic designs for algae dewatering

Microfluidic device	Optimum flow rate	Separation efficiency	Microalgae species, size	Reference

Trilobite Design	2 mL/min	30-60%	Rhodomonas baltica, 7 µm Chaetoceros, 5 µm	[28]
Asymmetric Serpentine	0.3 mL/min	96-98%	Synechocystis, 2 µm	[29]
Multiplexed Asymmetric Serpentine	0.5 mL/min	90%	Platymonas, 12 µm	[43]
Spiral	1.25 mL/min	84.4%	Platymonas, 12 µm	[30]
Rigid spiral microchannel	12 mL/min	99%	Tetraselmis suecica, 10 µm	This study

3.6 Conclusion

While microfluidics has showcased as an alternative method of microalgae harvesting, most of the devices were limited in working efficiency and throughput. In this study, by designing a modified spiral microfluidic channel, we increased the throughput dramatically while maintaining a high recovery efficiency of more than 99%. Our proposed microfluidic channel's operational flow rate of 12 mL/min is 40 times faster than the previously reported microfluidic device, with similar recovery efficiency of 96-98% [29]. There is also room to upscale the throughput by multiplexing the spiral channel. This demonstrates the tremendous potential of using this channel design on an industrial scale to physically process commercial photobioreactors in a short time, with high recovery efficiency and low risk of biomass deterioration.

4 Acknowledgment

The authors would also like to thank the Climate Change Cluster (C3) and the Faculty of Science at University of Technology Sydney (UTS) for their financial support.

List of figures

Fig. 1 The schematic workflow of the algae dewatering technique used in this study via spiral microfluidics. The spiral microchannel is made by 3D printing technique, in particular, stereolithography. Therefore, the microchannel is rigid.

Fig. 2 A) Particle focusing behaviour via wide ranges of flow rates. For 5 µm particles, they cannot form a tight focusing band near the channel outer wall and are partially focused at the outer wall for all flow rates. From 7 µm particles, at 2 mL/min, particles are mostly dispersed but from flow rate 6 mL/min onwards, particles perfectly focused at the channel outer wall, with separation efficiency more than 90% for flow rate of 6 mL/min and more than 95% for flow rate of 10 and 12 mL/min. 10 µm particles at 2 mL/min have better focusing performance compared to 7 µm particles where most of the particles are focused at the channel outer wall. Separation efficiency for 4 mL/min is ~ 80% and for 8 mL/min onwards it reaches more than 95%. For 15 µm particles, they are initially dispersed, more toward the channel inner wall. By increasing the flow rate, particles are migrating toward the channel outer wall where for 10 and 12 mL/min, particles are completely focused at the channel outer wall with separation efficiency more than 95%. The normalised intensity demonstrates the positioning of the particles within the channel width. B) separation efficiency for 5, 7, 10 and 15 µm particle at wide ranges of flow rates, from 2 to 12 mL/min. (The values are expressed as Mean ± SD, N=3)

Fig. 3 Effect of input denisty on the microchannel performance. Three different densities of 0.01, 0.1, and 1% v/v have been tested, the fluorescent streaks, normalised intensities, and overlayed-focusing images of particle movement have been demonstrated. The results revealed that the microchannel has the capacity to process samples at high density as well as perform multi-step concentrating

Fig. 4 *Tetraselmis* sp. microalgae dewatering. A) stacked image of *Tetraselmis* sp. species at different flow rates. Focusing behavior of the *Tetraselmis* sp. begins from the inner wall to the outer wall where for flow rates more than 6 mL/min, more than 90% of particles are focused at the outer wall and for 10 and 12 mL/min, it reaches ~99%. B) recovery efficiency of *Tetraselmis* sp. at different flow rates. C) to investigate the shear stress applied on the cells, the photosynthetic activity of the *Tetraselmis* sp. over different flow rates compared to the control sample has been evaluated. The results make it clear that the microchannel and the high operational flow rate do not induce additional force or stress on the algae samples. (The values are expressed as Mean ± SD, N=3)

Fig. 5 A) Experimental setup to harvest algae samples. B) Input sample of the *Tetraselmis* sp., target outlet (cell-rich fluid), waste outlet (cell-free fluid). C) channel overview at the flow rate of 12 mL/min. D) loop-by-loop investigation of the focusing position of the particles. (The values are expressed as Mean ± SD, N=3) (P value > 0.05)

Fig. 6 The possibilities of scaling up the microfluidic system illustrated in this study via A) vertical B) planar multiplexing.

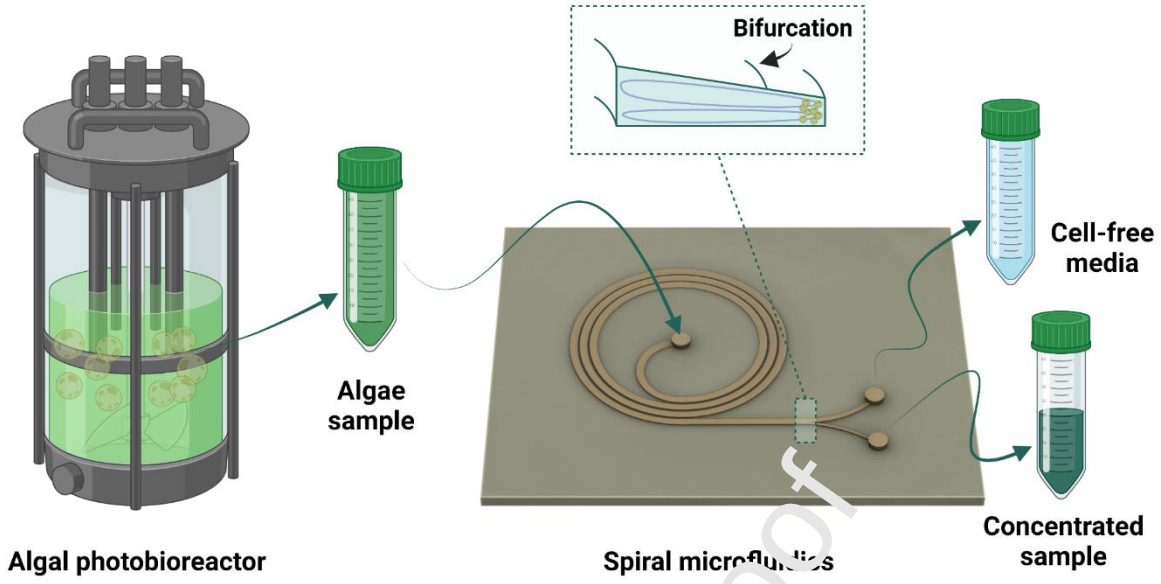

Fig. 1

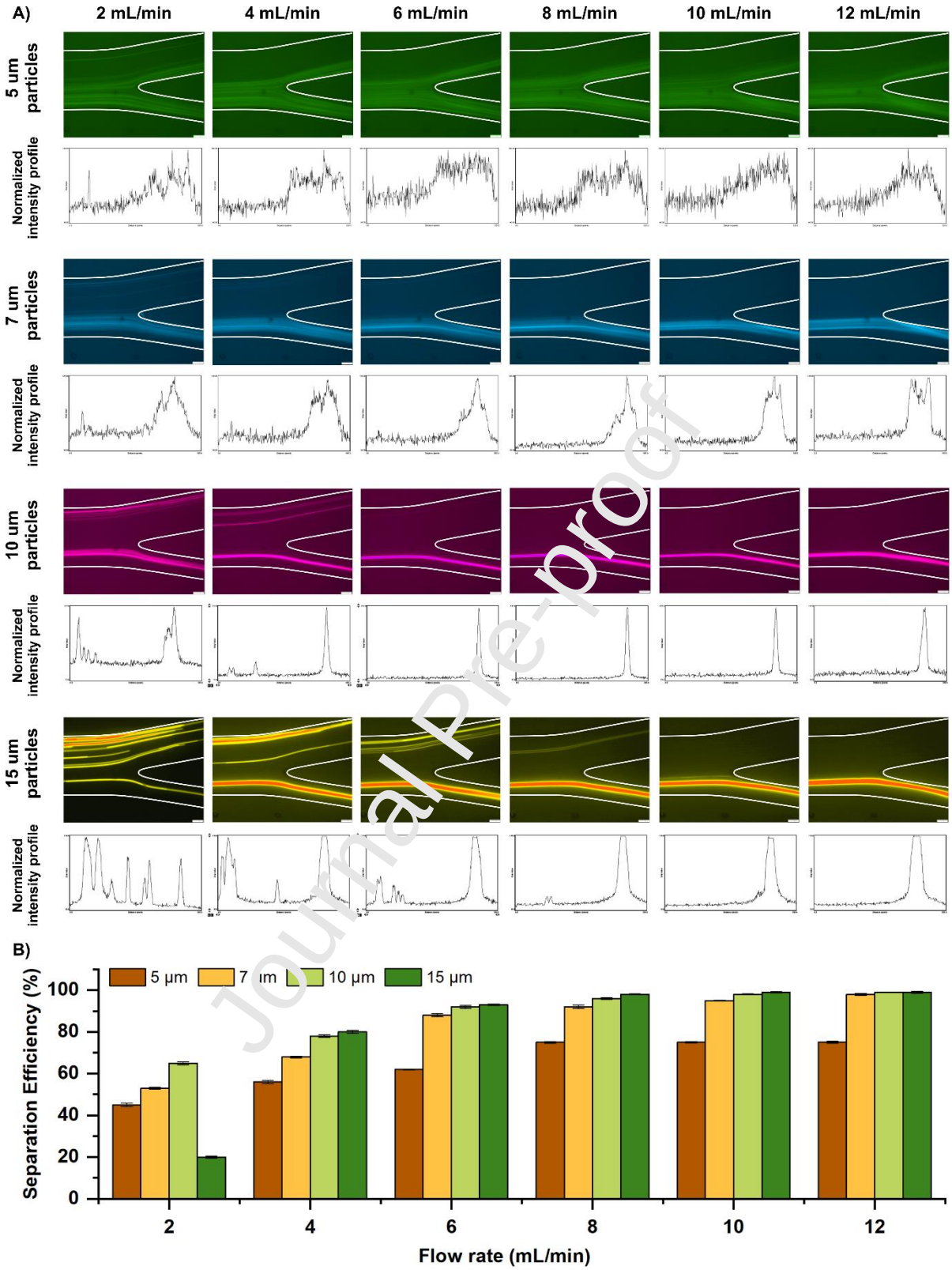

Fig. 2

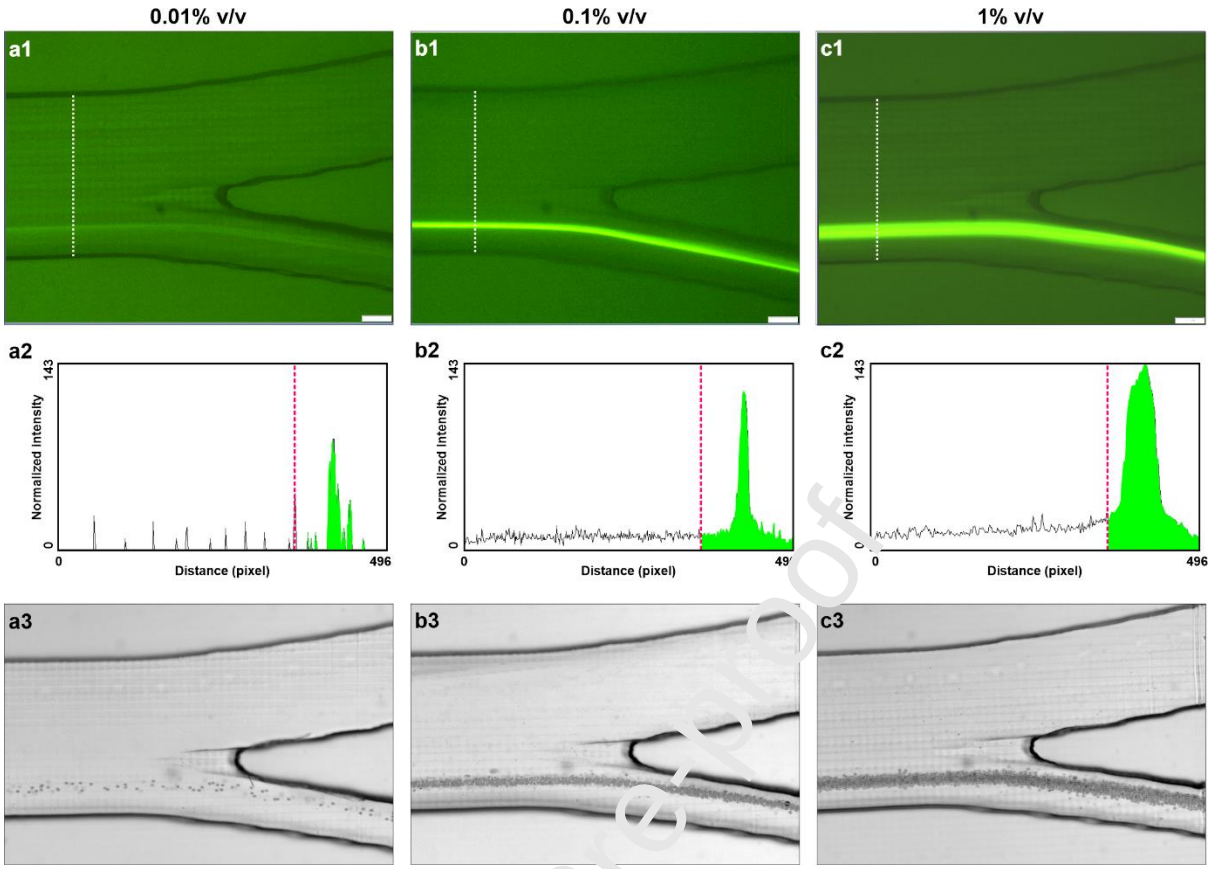

Fig. 3

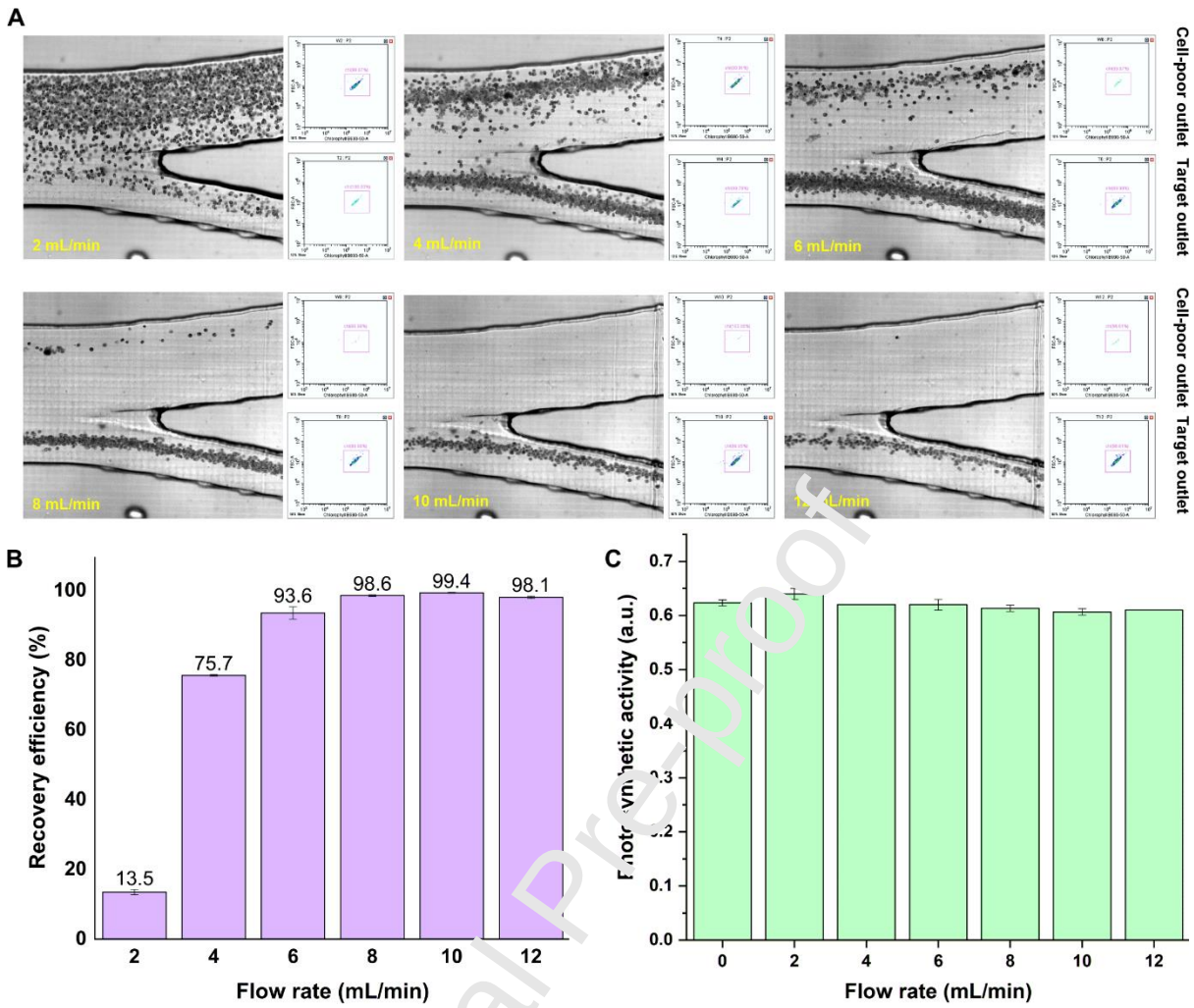

Fig. 4

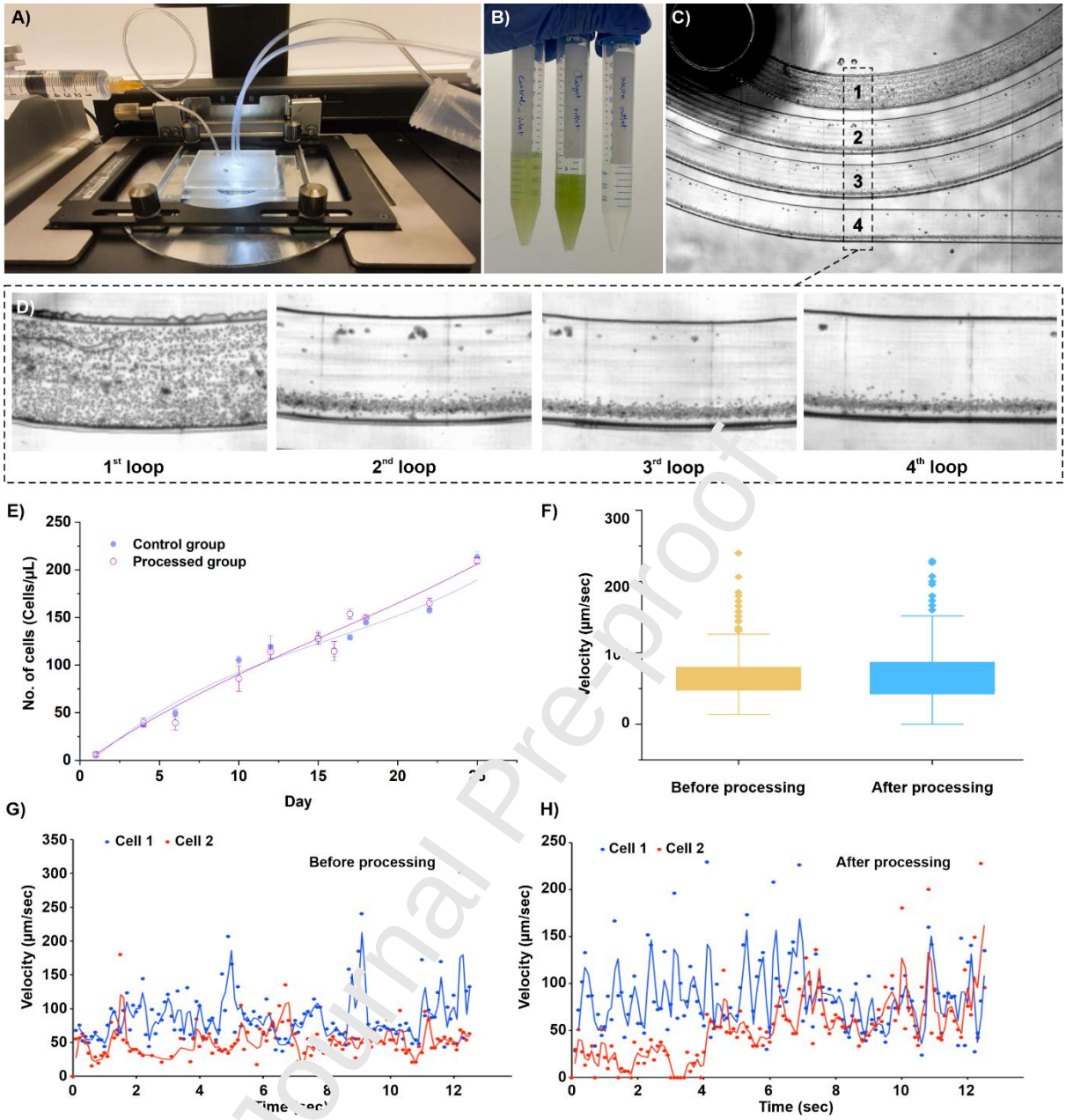

Fig. 5

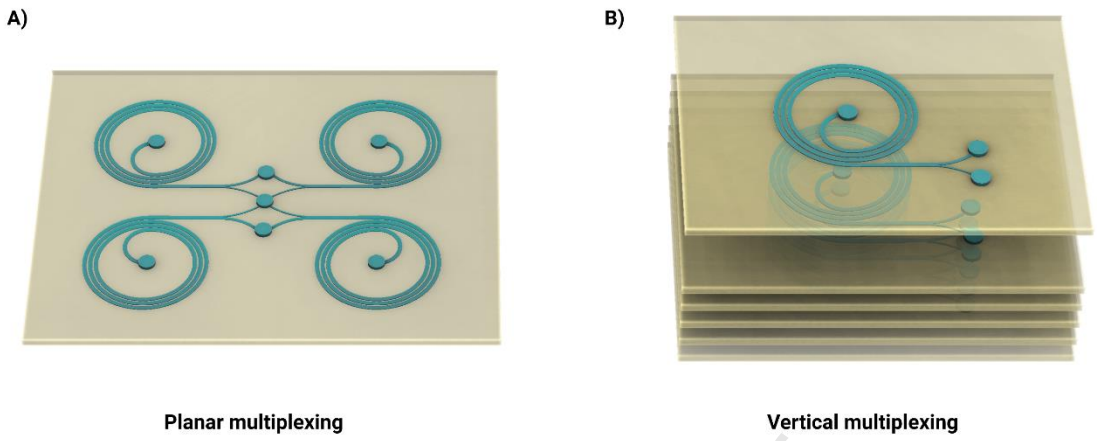

Fig. 6

References

[1] A. L. Ahmad, N. H. M. Yasin, C. J. C. Derek, and J. K. Lim, "Microalgae as a sustainable energy source for biodiesel production: A review," *Renewable and Sustainable Energy Reviews,* vol. 15, no. 1, pp. 584-593, 2011/01/01/ 2011, doi: https://doi.org/10.1016/j.rser.2010.09.018.

[2] D. H. P. Ng, Y. K. Ng, H. Shen, and Y. K. Lee, "Chapter 6 - Microalgal Biotechnology: The Way Forward," in *Handbook of Marine Microalgae*, S.-K. Kim Ed. Boston: Academic Press, 2015, pp. 69-80.

[3] L. Barsanti and P. Gualtieri, "Is exploitation of microalgae economically and energetically sustainable?," *Algal Research,* vol. 31, pp. 107-115, 2018/04/01/ 2018, doi: https://doi.org/10.1016/j.algal.2018.02.001.

[4] R. U. Tanvir, J. Zhang, T. Canter, D. Chen, J. Lu, and Z. Hu, "Harnessing solar energy using phototrophic microorganisms: A sustainable pathway to bioenergy, biomaterials, and environmental solutions," *Renewable and Sustainable Energy Reviews,* vol. 146, p. 111181, 2021/08/01/ 2021, doi: https://doi.org/10.1016/j.rser.2021.111181.

[5] G. B. Leite, A. E. M. Abdelaziz, and P. C. Hallenbeck, "Algal biofuels: Challenges and opportunities," *Bioresource Technology,* vol. 145, pp. 134-141, 2013/10/01/ 2013, doi: https://doi.org/10.1016/j.biortech.2013.02.007.

[6] R. Chandra, H. M. N. Iqbal, G. Vishal, H.-S. Lee, and S. Nagra, "Algal biorefinery: A sustainable approach to valorize algal-based biomass towards multiple product recovery," *Bioresour. Technol.,* vol. 278, pp. 346-359, 2019/04/01/ 2019, doi: https://doi.org/10.1016/j.biortech.2019.01.104.

[7] A. I. Barros, A. L. Gonçalves, M. Simões, and J. C. M. Pires, "Harvesting techniques applied to microalgae: A review," *Renewable and Sustainable Energy Reviews,* vol. 41, pp. 1489-1500, 2015/01/01/ 2015, doi: https://doi.org/10.1016/j.rser.2014.09.037.

[8] E. Molina Grima, E. H. Belarbi, F. G. Acién Fernández, A. Robles Medina, and Y. Chisti, "Recovery of microalgal biomass and metabolites: process options and economics," *Biotechnol. Adv.,* vol. 20, no. 7, pp. 491-515, 2003/01/01/ 2003, doi: https://doi.org/10.1016/S0734-9750(02)00050-2.

[9] M. K. Danquah, B. Gladman, N. Moheimani, and G. M. Forde, "Microalgal growth characteristics and subsequent influence on dewatering efficiency," *Chem. Eng. J.,* vol. 151, no. 1, pp. 73-78, 2009/08/15/ 2009, doi: https://doi.org/10.1016/j.cej.2009.01.047.

[10] M. Roy and K. Mohanty, "A comprehensive review on microalgal harvesting strategies: Current status and future prospects," *Algal Research,* vol. 44, p. 101683, 2019/12/01/ 2019, doi: https://doi.org/10.1016/j.algal.2019.101683.

[11] G. M. Whitesides, "The origins and the future of microfluidics," *Nature,* 10.1038/nature05058 vol. 442, no. 7101, pp. 368-373, 07/27/print 2006. [Online]. Available: http://dx.doi.org/10.1038/nature05058.

[12] F. Mirakhorli, S. S. Mohseni, S. R. Bazaz, A. A. Mehrizi, P. J. Ralph, and M. E. Warkiani, "Microfluidic Platforms for Cell Sorting," in *Sustainable Separation Engineering*, 2022, pp. 653-695.

[13] D. Di Carlo, "Inertial microfluidics," *Lab on a Chip,* vol. 9, no. 21, pp. 3038-3046, 2009.

[14] S. Razavi Bazaz, A. Mashhadian, A. Ehsani, S. C. Saha, T. Krüger, and M. Ebrahimi Warkiani, "Computational inertial microfluidics: a review," *Lab on a Chip,* 10.1039/C9LC01022J vol. 20, no. 6, pp. 1023-1048, 2020, doi: 10.1039/C9LC01022J.

[15] C. Lei *et al.*, "High-throughput imaging flow cytometry by optofluidic time-stretch microscopy," *Nature Protocols,* vol. 13, no. 7, pp. 1603-1631, 2018/07/01 2018, doi: 10.1038/s41596-018-0008-7.

[16] J. Shrestha *et al.*, "Rapid separation of bacteria from primary nasal samples using inertial microfluidics," *Lab on a Chip,* 10.1039/D2LC00794K vol. 23, no. 1, pp. 146-156, 2023, doi: 10.1039/D2LC00794K.

[17] A. Mihandoust, S. Razavi Bazaz, N. Maleki-Jirsaraei, M. Alizadeh, R. A. Taylor, and M. Ebrahimi Warkiani, "High-Throughput Particle Concentration Using Complex Cross-Section Microchannels," *Micromachines,* vol. 11, no. 4, p. 440, 2020. [Online]. Available: https://www.mdpi.com/2072-666X/11/4/440.

[18] H. S. Kim, T. P. Devarenne, and A. Han, "Microfluidic systems for microalgal biotechnology: A review," *Algal Research,* vol. 30, pp. 149-161, 2018/03/01/ 2018, doi: https://doi.org/10.1016/j.algal.2017.11.020.

[19] G. Benazzi, D. Holmes, T. Sun, M. C. Mowlem, and H. Morgan, "Discrimination and analysis of phytoplankton using a microfluidic cytometer," *IET Nanobiotechnology*, vol. 1, no. 6, pp. 94-101. [Online]. Available: https://digital-library.theiet.org/content/journals/10.1049/iet-nbt_20070020

[20] Y.-L. Deng, M.-Y. Kuo, and Y.-J. Juang, "Development of flow through dielectrophoresis microfluidic chips for biofuel production: Sorting and detection of microalgae with different lipid contents," *Biomicrofluidics,* vol. 8, no. 6, p. 064120, 2014/11/01 2014, doi: 10.1063/1.4903942.

[21] Y.-L. Deng, J.-S. Chang, and Y.-J. Juang, "Separation of microalgae with different lipid contents by dielectrophoresis," *Bioresour. Technol.,* vol. 135, pp. 137-141, 2013/05/01/ 2013, doi: https://doi.org/10.1016/j.biortech.2012.11.046.

[22] S. Abalde-Cela, A. Gould, X. Liu, E. Kazamia, A. G. Smith, and C. Abell, "High-throughput detection of ethanol-producing cyanobacteria in a microdroplet platform," *Journal of The Royal Society Interface,* vol. 12, no. 106, p. 20150216, 2015/05/06 2015, doi: 10.1098/rsif.2015.0216.

[23] H. S. Kim, T. P. Devarenne, and A. Han, "A high-throughput microfluidic single-cell screening platform capable of selective cell extraction," *Lab on a Chip,* 10.1039/C4LC01316F vol. 15, no. 11, pp. 2467-2475, 2015, doi: 10.1039/C4LC01316F.

[24] P. J. Graham, J. Riordon, and D. Sinton, "Microalgae on display: a microfluidic pixel-based irradiance assay for photosynthetic growth," *Lab on a Chip,* 10.1039/C5LC00527B vol. 15, no. 15, pp. 3116-3124, 2015, doi: 10.1039/C5LC00527B.

[25] H. S. Kim, T. L. Weiss, H. R. Thapa, T. P. Devarenne, and A. Han, "A microfluidic photobioreactor array demonstrating high-throughput screening for microalgal oil production," *Lab on a Chip,* 10.1039/C3LC51396C vol. 14, no. 8, pp. 1415-1425, 2014, doi: 10.1039/C3LC51396C.

[26] H. S. Lim, J. Y. H. Kim, H. S. Kwak, and S. J. Sim, "Integrated Microfluidic Platform for Multiple Processes from Microalgal Culture to Lipid Extraction," *Anal. Chem.,* vol. 86, no. 17, pp. 8585-8592, 2014/09/02 2014, doi: 10.1021/ac502324c.

[27] H. S. Kwak, J. Y. H. Kim, S. C. Na, N. L. Jeon, and S. J. Sim, "Multiplex microfluidic system integrating sequential operations of microalgal lipid production," *Analyst,* 10.1039/C5AN02409A vol. 141, no. 4, pp. 1218-1225, 2016, doi: 10.1039/C5AN02409A.

[28] B. K. Hønsvall, D. Altin, and L. J. Robertson, "Continuous harvesting of microalgae by new microfluidic technology for particle separation," *Bioresour. Technol.,* vol. 200, pp. 360-365, 2016/01/01/ 2016, doi: https://doi.org/10.1016/j.biortech.2015.10.046.

[29] L. Wang and D. S. Dandy, "A microfluidic concentrator for cyanobacteria harvesting," *Algal Research,* vol. 26, pp. 481-489, 2017/09/01/ 2017, doi: https://doi.org/10.1016/j.algal.2017.03.018.

[30] N. Xiang *et al.*, "Low-cost multi-core inertial microfluidic centrifuge for high-throughput cell concentration," *ELECTROPHORESIS,* vol. 41, no. 10-11, pp. 875-882, 2020, doi: https://doi.org/10.1002/elps.201900385.

[31] S. Razavi Bazaz *et al.*, "3D Printing of Inertial Microfluidic Devices," *Scientific Reports,* vol. 10, no. 1, p. 5929, 2020/04/03 2020, doi: 10.1038/s41598-020-62569-9.

[32] S. Razavi Bazaz, "3D Printing for Microfluidics," 2022.

[33] R. Salomon, S. Razavi Bazaz, W. Li, D. Gallego-Ortega, D. Jin, and M. E. Warkiani, "A Method for Rapid, Quantitative Evaluation of Particle Sorting in Microfluidics Using Basic Cytometry Equipment," *Micromachines*, vol. 14, no. 4, doi: 10.3390/mi14040751.

[34] S. Macdonald Miller, R. M. Abbriano, A. Segecova, A. Herdean, P. J. Ralph, and M. Pernice, "Comparative Study Highlights the Potential of Spectral Deconvolution for Fucoxanthin Screening in Live Phaeodactylum tricornutum Cultures," *Mar Drugs,* vol. 20, no. 1, 2022, doi: 10.3390/md20010019.

[35] M. E. Larsson *et al.*, "Mucospheres produced by a mixotrophic protist impact ocean carbon cycling," *Nature Communications,* vol. 13, no. 1, p. 1301, 2022/03/14 2022, doi: 10.1038/s41467-022-28867-8.

[36] G. Zheng *et al.*, "Development of Microfluidic Dilution Network-Based System for Lab-on-a-Chip Microalgal Bioassays," *Analytical Chemistry,* vol. 90, no. 22, pp. 13280-13289, 2018/11/20 2018, doi: 10.1021/acs.analchem.8b02597.

[37] S. Sinutok, R. Hill, M. A. Doblin, and P. J. Ralph, "Diurnal photosynthetic response of the motile symbiotic benthic foraminiferan Marginopora vertebralis," *Marine Ecology Progress Series,* vol. 478, pp. 127-138, 2013. [Online]. Available: https://www.int-res.com/abstracts/meps/v478/p127-138.

[38] J. Zhou and I. Papautsky, "Fundamentals of inertial focusing in microchannels," *Lab on a Chip,* vol. 13, no. 6, pp. 1121-1132, 2013.

[39] S. Razavi Bazaz *et al.*, "Zigzag microchannel for rigid inertial separation and enrichment (Z-RISE) of cells and particles," *Lab on a Chip,* 10.1039/D2LC00290F vol. 22, no. 21, pp. 4093-4109, 2022, doi: 10.1039/D2LC00290F.

[40] S. Razavi Bazaz, S. Zhand, R. Salomon, E. M. Beheshti, D. Jin, and M. E. Warkiani, "ImmunoInertial microfluidics: A novel strategy for isolation of small EV subpopulations," *Applied Materials Today,* vol. 30, p. 101730, 2023/02/01/ 2023, doi: https://doi.org/10.1016/j.apmt.2022.101730.

[41] E. Sollier, C. Murray, P. Maoddi, and D. D. Carlo, "Rapid prototyping polymers for microfluidic devices and high pressure injections," *Lab on a Chip,* vol. 11, no. 22, pp. 3752-3765, 2011.

[42] B. L. Khoo *et al.*, "Clinical validation of an ultra high-throughput spiral microfluidics for the detection and enrichment of viable circulating tumor cells," *PloS one,* vol. 9, no. 7, p. e99409, 2014.

[43] N. Xiang, R. Zhang, Y. Han, and Z. Ni, "A Multilayer Polymer-Film Inertial Microfluidic Device for High-Throughput Cell Concentration," *Anal. Chem.,* vol. 91, no. 8, pp. 5461-5468, 2019/04/16 2019, doi: 10.1021/acs.analchem.9b01116.

CRediT authorship contribution statement

F.M: Methodology, Software, Validation, Formal analysis, Investigation, Writing – original draft, Writing - Review & Editing, Visualization

S.R.B: Methodology, Validation, Writing – original draft, Writing - Review & Editing,

M.E.W: Resources, Writing - Review & Editing

P.J.R: Resources, Data Curation, Supervision, Writing - Review & Editing, Project administration

Declaration of interests

☒The authors declare that they have no known competing financial interests or personal relationships that could have appeared to influence the work reported in this paper.

☐The authors declare the following financial interests/personal relationships which may be considered as potential competing interests:

Highlights

- Harvesting is an inseparable costly process in the algae-related industry.
- A high-throughput microfluidic device is designed based on rigid materials.
- The microfluidic device can robustly separate a wide range of microalgae species at high flow rates and recovery efficiency.
- A promising alternative for microalgae dewatering enabling low-cost processing of commercial photobioreactors with low risk of biomass deterioration and contamination.